

Dynamics of atmospheric aerosol, ions, and trace gases at invasion of the arctic air masses

V.V. Smirnov,¹ J. Salm,² J.M. Mäkelä,³ and J. Paatero⁴

¹ *Institute of Experimental Meteorology, Obninsk, Russia*

² *Institute of Environmental Physics, Tartu University, Tartu, Estonia*

³ *Institute of Physics, University of Technology, Tampere, Finland*

⁴ *Institute of Meteorology, Helsinki, Finland*

Received October 14, 2003

Within the ESUP International Experiment carried out in March–April 2000 in Southern Finland, the correlations were found, for the first time, between the burst generation of ultrafine condensation nuclei (from 3 to 10 nm in diameter) and the concentrations of light, intermediate, and heavy ions, as well as NO, NO_x, SO_x, O₃, CO₂, and radon gases, and atmospheric aerosols in the size range of 10 nm to 10 μm, the state of meteorological elements in the near-ground atmospheric layer, and other parameters. These correlations allow better understanding of the phenomenon observed.

Introduction

The series of regular observations of earlier unknown atmospheric phenomenon of an intense emission of nanometer-size aerosol particles and their subsequent growth occurring in some synoptic situations, are presented in Refs. 12, 21, 24, 30, etc.

The term “nucleation burst” (NB) is used in English literature for description of this phenomenon. Revealing of the nature and significance of NB was the object of a number of European projects, in particular, EUROFLUX³⁰ and BIOFOR.^{15,16,21} In spite of a significant complex of physical, meteorological, and biochemical researches, the mechanisms of NB and its relations to other processes have not yet been revealed. There were also many unclear details in understanding another one phenomenon, an intense emission of intermediate (II) and heavy (HI) atmospheric ions in the near-ground atmosphere.^{18,23,25}

The primary purpose of this paper was to summarize the results obtained during the comprehensive international experiment ESUP-2000 (Electrical State of Ultrafine Particles) carried out in March–April 2000 in Southern Finland. The site of the experiment was in Hiitila, a forestry station situated 230 km north of Helsinki, where a unique experimental complex¹⁷ SMEAR II was designed on the basis of gradient meteorological mast with the measurement levels at 4, 16, and 67 m for a comprehensive study of the boundary layer, forest micrometeorology, atmospheric aerosols and trace gases. The experiments were focused on revealing the relations between the variations of aerosol concentration in a wide size range (from 3 nm to 10 μm), atmospheric ions of different mobility ($u = 5 - 5 \cdot 10^{-3} \text{ cm}^2/\text{V} \cdot \text{s}$), and gases (O₃, NO, NO_x, SO_x, and CO₂) in the near-ground layer of the atmosphere. It was planned to estimate the role of photochemical and electric processes in the formation of aerosol substance in the atmosphere and the effect of NB on the electric state of the atmosphere on the basis of these and accompanying meteorological data.

1. Instrumentation and techniques

An ALSI-1 meter intended for spectrometry of ions with the mobility from 3 and down to 0.1 cm²/V · s was designed on the basis of a UT-8515 differential aspiration six-channel aeroion counter.¹⁹ Then the device was adapted to continuous computer-controlled monitoring of the mobility spectrum of light and intermediate ions.²⁸ The sampling has been done at a rate about 2000 cm³/s through a 1-m long and 10-cm diameter metal tube. The duration of measurements of an individual spectrum was about 5 minutes. The intervals between successive measurements for this and other devices are given in Table 1.

Number densities of light, intermediate, and heavy ions were determined by means of four universal integral aeroion counters of UT-8401 type united in an aspiration network.¹⁹ The duration of a single measurement cycle was 10 minutes. The polar electroconductivity of the air was determined continuously by means of a classic aeroion meter of the Herdian type.¹³

The DAES-2 electric aerosol analyzer²⁹ was used for measuring the size spectrum and number density of particles in the size range from $D = 5 \text{ nm}$ to $1 \mu\text{m}$. Its operation principle is as follows: unipolar charging of aerosol, selection of charged aerosols by mobility, and measurement of the ion current by the Faraday method. The aerosol volume rate was up to 250 cm³/s.

Together with other devices the DAES-2 analyzer was operated in a separate building in a forest zone. The samples were collected round-the-clock at the height about 2 m above the ground. Four personal computers were used for the measurement control and data storage. The coarse particle size spectrum ($D = 0.5 - 5 \mu\text{m}$) was detected by means of a PC-218 Royco Instr. Co., USA, photoelectric counter with a filament lamp as illuminator and a photodiode to detect light scattered forward at 5 to 30° scattering angle. The intensity of electric field was estimated occasionally from the readouts of the INEP rotating

Table 1. Experimentally measured ESUP characteristics of the near-ground atmosphere

Element	Notation	Mobility, $\text{cm}^2/\text{V} \cdot \text{s}$	Diameter, nm	Meter	Operator
Light ions	n_-	0.35–5	1.9–0.5	Ion counter UT8401 – 4 devices	Estonia
	n_-, n_+	0.9–3.2	1.6–0.6	Spectrometer ALSI-1	Russia
	C_-, C_+	2– ∞		Meter of electroconductivity of the Herdien type	Finland
Intermediate ions	m_-	0.035–0.35	7.4–1.9	Aeroion counter UT8401	
	M_-, M_+	0.12–0.9	3.5–1.6	Ion spectrometer ALSI-1	
Heavy ions	N_-	0.005–0.035	20–7.4	Ion counter UT8401	
Aerosol	N_-, N_a	$0.25-2.5 \cdot 10^{-5}$	3–500	Spectrometer DMPS	Finland
	N_a		$5 \cdot 10^3$	Electric analyzer DAES-2	Russia
	N_a		$500-5 \cdot 10^3$	Counter PC-218 Royco Inc., USA	Russia
Electric field	E_z	$E_z = 20-1000 \text{ V/m}$		Strength meter INEP	Russia

fluxmeter in the range from 20 to $\pm 1000 \text{ V/m}$. The INEP sensor was installed on an open plate 20 m far from the building.

Other meters and sensors were arranged in the building of the aforementioned station SMEAR II at the distance of 450 m. The DMPS system of two differential analyzers of electric mobility of the Hauke type³³ was used here for analysis of the aerosol dispersity $D = 3-25$ and 20–500 nm. The aerosol flow rate was 2.5 l/min. The particles separated by mobility came to the condensation nuclei counters TSI–3025 and TSI–3010. The actual measurement cycle within the entire size range $D = 3$ to 500 nm was about 10 min. The sampling was done at a height of 2 m. The radon content in air was recorded continuously by the method of counting β -particles emitted by radon daughter products settled on aerosol particles. Aerosol particles were settled on a filter. The inlet of air sampling device was set at the height of 6 m above the ground.

2. Micrometeorology and synoptic data

The results of aforementioned investigations (for example, Refs. 12 and 21) show that the NB effect is observed approximately equally: at about noon the number density of aerosol particles of the size $D = 3$ to 10 nm increases during about some tens of minutes from units or tens to some thousand and even tens thousand particles per 1 cm^3 . Then in 70–80% of events the growth of the nucleation mode $D = 3$ to 20 nm and the Aitken mode $d = 40$ to 80 nm occurs during the time of about few hours. These processes weaken by the evening. The common natural conditions for appearance

of new particles were the absence of cloudiness and coming of air masses with moderate wind from north. These features are confirmed in this cycle of experiments, but a number of new peculiarities have been revealed during the joint analysis of atmospheric electric, aerosol, and micrometeorological data.

Synoptic situation. One can see in Table 2 and in Fig. 1 that the following meteorological conditions precede the nucleation bursts: moving of air masses from north-west, mean values of near-ground wind velocity and azimuth, respectively, $(4 \pm 1) \text{ m/s}$ and $(235 \pm 20)^\circ$, clear sky weather characteristic of spring anticyclones in snow-covered regions, morning near-surface inversions, and significant diurnal temperature change from -10 to $\approx +5^\circ\text{C}$ at night and from $+3$ to $+7^\circ\text{C}$ at noon with the relative humidity of air 60–70 and 30–45%, respectively.

The investigations carried out in the frameworks of the BIOFOR project in 1999–2000 have shown^{21,22} that the NB episodes in Southern Finland occurred in the back of cold fronts and only occasionally in the back of occlusion fronts. For a detailed consideration of the macrosynoptic situation we analyzed the TV images obtained from the NOAA–14 satellite kindly presented by the Institute of Space Research RAS. The circumpolar circulation of air masses characteristic of this season, which formed the moderate northwest winds in the near-ground layer, was observed.

The back 24-hour trajectories were estimated using the technique taking into account the results^{2,3} for the characteristic forecast situations with pressure and wind fields. These trajectories started in the regions of northern Arctic with the probability of 80% that, in general, confirms and refines the conclusions drawn in Ref. 21.

Table 2. Characteristic atmospheric electric parameters of air at Hiitjala Obs., Finland, since March 24 until April 15, 2000. The parameters in days with NB are averaged over 1 hour before NB, in other days – over the period since 10 a.m. until noon

Days	Number of days	Time of beginning t_0 , h	Duration, t , h	Wind azimuth, deg.	C , fCm/m	E_z , V/m	[SO ₂], billion ⁻¹	[NO ₂], billion ⁻¹	N_0 , cm ⁻³ $D > 3 \text{ nm}$	N_m , cm ⁻³ $D > 3 \text{ nm}$	N_m/N_0	N_a , cm ⁻³ $D > 0.5 \mu\text{m}$
All	24	10		225	10	120	0.45	2	1500	4100	3	2.4
With NB	17	10.5	7.3	237	12.3	220	0.4	1.9	1517	6835	4.5	1.87
Without NB	7	0		200	10.6	70	0.68	2.9	2000	2200	2.1	4.5

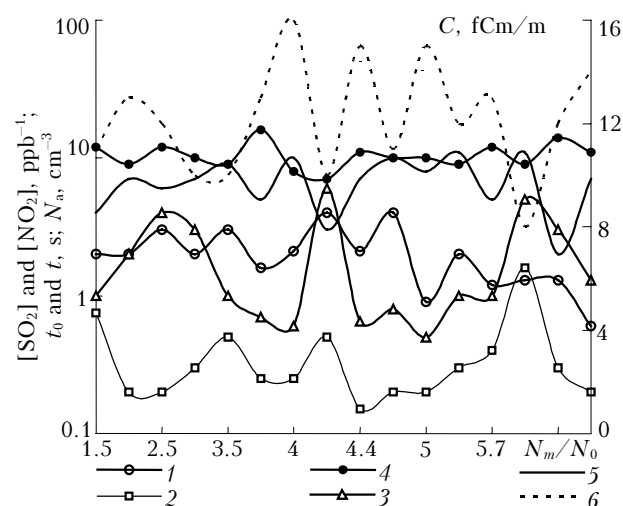


Fig. 1. Maximum increase of the number density of new particles N_m/N_0 as a function of the atmospheric parameters preceding NB. Here and below at Hiitila Obs.: number density of coarse aerosol N_a (1); concentrations of gases NO_2 and SO_2 (2 and 3); time of appearance t_0 and duration of emissions t (4 and 5); mean electric conductivity of air C (right scale) (6).

Spatial scale of the phenomenon. It follows from analysis of data presented in Refs. 3 and 14 that the peculiar circulation is statistically characteristic of the Northern Europe in March–April and September–March, when Arctic is isolated by cloud fields of the western cycle from Greenland to Murmansk and by the lane of clear sky of the width of about 500 km. This lane widens over the territory of Russia to 2000 km reaching the regions to the east from the line Kazan’–Astrakhan’. The mesoscale vortices periodically move along this corridor. In particular, the Azor–Greenland anticyclone characteristic of spring and fall moved along this direction with the period of 6–7 days playing the role of a valve transmitting the portions of clean and moderately cold ocean air. Obviously, such a synoptic situation observed every year in March–April is well reproducible. The streams move along this corridor with low velocities and vertical gradients, because cloud fraction is small, but heating in the daytime and the intensity of exchange processes are essential. One can only expect with some certainty that distortions of aerosol and ion components of the atmosphere similar to that observed in the Southern Finland have synoptic scale and should be observed over all Northern Europe.

Seasonal or annual cycle. Seasonal factors of NB in 1996–1999 were well pronounced: maxima in transitional seasons (on the average, 8 to 10 events in March–April with the peak value of the number density $N = 6 \cdot 10^3$ – 10^4 cm^{-3} and 4 to 7 events in September and October). Minima of NB were observed in August (1–2 events of $N = 2 \cdot 10^3 \text{ cm}^{-3}$) and December (0–1 event).^{22,30} The monthly average behavior of the number of NB and peak aerosol number density in 1996 are shown in Fig. 2 as an example, as well as the data³² on the annual mean behavior of the

atmospheric ozone content. As is seen, the maxima of NB and N_m are observed in spring and fall, the maxima of N_m are shifted to the colder months, March and October. The probability of bursts in August and December is low.

Fig. 2. Monthly variations of the quantity (1) of intensive nucleation bursts NB, peak number density (2) of aerosols³⁰ N_m , and the total ozone content (3) in Dobson units from the data of 68 ground-based stations of the Northern Hemisphere.³²

Diurnal cycle. As is seen, nucleation bursts are observed only in daytime, i.e., they have the well-pronounced diurnal behavior. The beginning and duration of NB vary within a sufficiently wide range, then it is reasonable to consider in a more detail the data of most characteristic days.

Figure 3 presents the event of an intense NB observed under conditions of a sufficiently stable wind direction (the azimuth at noon was 220° , and in the morning and in the evening it was 260°). The fact attracted our attention that the maxima of total GR = 500 W/m^2 and ultraviolet UV-A = 30 W/m^2 and UV-B = 0.8 W/m^2 fluxes of solar radiation were observed at noon. The minimum of the radon content as well as the maximum of the negative temperature gradient $dT = -0.02^\circ\text{C}$ usually accompanied them, and it is an evidence of reaching the mixing maximum in the near-ground layer. The maxima of the near-ground wind velocity at the level of 17 m $u = 6 \text{ m/s}$ and temperature $+3^\circ\text{C}$, as well as the minimum of relative humidity $H = 37\%$ were shifted in time approximately by 3 hours. The maxima of the number density of new aerosol particles N and intermediate ions M were reached at 3 p.m.

3. Dynamics of trace gases, aerosols, and ions

3.1. Trace gases

It has been experimentally revealed that some atmospheric gases at certain concentration relationships stimulate the formation of natural and anthropogenic smog (see, for example, Ref. 1). Hence,

one could expect to obtain a decisive contribution to the study of NB genesis in analyzing the variations of aerosols and such trace gases as SO_2 , NO_x , NO , O_3 , CO_2 . Equipment of the SMEAR II station made it possible to measure the concentrations of these gases at three levels of 4.2, 16.8, and 67.2 m in a round-the-clock regime. The near-ground radon concentration was measured occasionally (see Fig. 3a). Let us note that the considered near-ground layer 4 to 70 m was

most often homogeneous in the daytime in the meaning of small value of the vertical gradients of SO_2 , NO_x , NO , O_3 , as well as of water vapor. It is an indication of the absence of local sources of these matters in the atmosphere. As was expected, the vertical behavior of carbon dioxide concentration was noticeable over forest. Its concentration was maximum at 4 m (385 ppm) with the vertical gradient of 0.5 ppm per every 10 m.

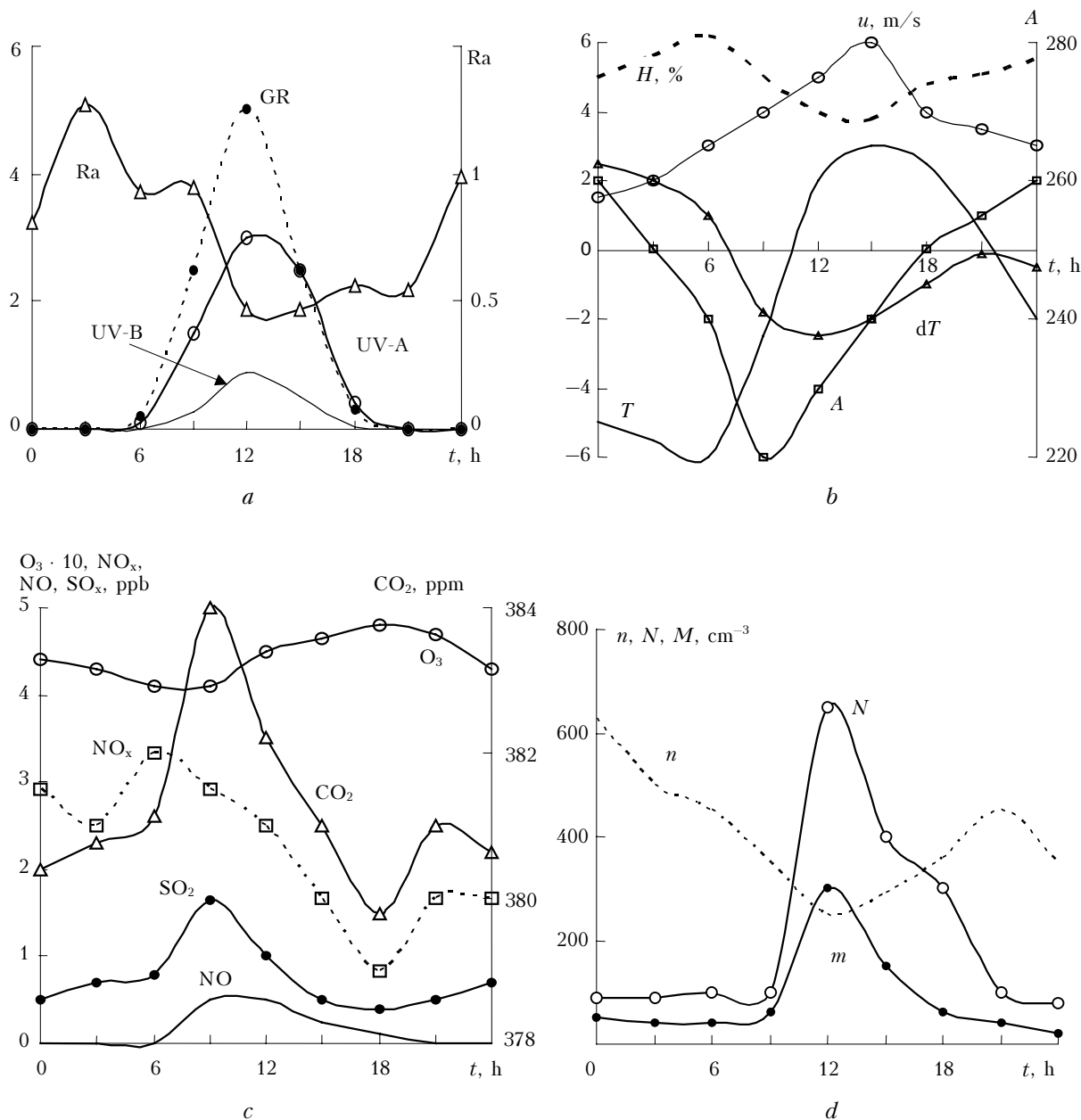


Fig. 3. Variations of radiative (a), thermal (b), gaseous (c), and ion (d) characteristics of the near-ground atmosphere during a day on March 29, 2000. GR is the global radiation; UV-A and UV-B are the A and B UV-components; u and A are the wind velocity and direction at the height of 16 m; T , dT , and H are, respectively, temperature, its gradient, and relative humidity at the height of 16 m; O_3 , CO_2 , NO , NO_x , SO_2 are the concentrations of ozone, carbon dioxide, nitrogen and sulfur oxides at the height of 4 m; n , M , and N , respectively, are the number densities of light, intermediate, and heavy negative ions at the height of 2 m; Ra is radon concentration in rel. units.

Table 3. Mean concentrations of some gases (in ppb by mass) in the near-ground layer at Hiitila Obs. in 2000, as well as in mid-latitudes and in the polar region⁵

Type of gas	Hiitila Obs., all cases	Hiitila Obs., cases with NB *	Mid-latitudes	Polar latitudes
SO ₂	0.48 (0.25–2)**	0.38	0.2–5	0.002–0.02
NO	0–0.05 (0–0.8)			
NO ₂ ***	2.1 (1–5)	1.63	1–3	0.2–2
O ₃	41 (38–50)	43	20–40	15
CO ₂ , ppm	375–385			
OH, cm ⁻³			1.3 · 10 ⁶	5 · 10 ⁵

(*) Averaging over 3 hours before NB, (**) in parentheses is the interval of values with confidence probability 85%, (***) concentration of NO_x was measured at Hiitila Obs.

The results of measurements in all days and the days with NB are presented in Table 3. The data from Ref. 5 for polar and mid-latitudes were used for a comparison. As is seen in Table 3, the content of trace gases in the period before NB do not noticeably differ from both background and global values. Diurnal behavior of the ozone with maximum at 5–6 p.m. equal to 47–50 ppm and with the minimum of 40–43 ppm at 6 a.m. was quite usual for warm seasons of a year. The example of the record of the diurnal behavior of ozone and other gases is shown in Fig. 3c. The carbon dioxide concentration changed opposite to ozone that is characteristic of the region with active vegetation.

The nitrogen and sulfur oxides concentrations did not show any well pronounced diurnal behavior, therefore their peaks since 8 a.m. until noon in Fig. 3c were not typical and were not related to the behavior of meteorological parameters and number densities of aerosols and aeroions. Figure 3 is one more (see also Fig. 1 and Table 2) illustration of the fact that variations of the number density of new particles and aforementioned trace gases weakly correlate with each other. However, it is interesting why the concentrations of SO₂ and NO_x during NB were often 20% lower than before the episodes. Perhaps, the days with NB were characterized by invasion of arctic air masses, which have smaller concentration of trace gases (see Table 3). For a comparison, the mass concentration of SO₂ in the 60% of the observation time in 1992–95 in the Finnish part of Lapland did not exceed 1 ppb with the peaks in winter³¹ up to 2–3 ppb.

3.2. Atmospheric aerosol

Let us return to Table 2 and note that the mean peak number density of particles in the days with NB $N_m \approx 7 \cdot 10^3 \text{ cm}^{-3}$ exceeds the mean background value $N_0 \approx 1500 \text{ cm}^{-3}$ by 5 times, and in some days by 10–13 times. The duration of bursts varied from 3 to 10 hours when the number density N_m exceeded the mean near-ground “aerosol” background N_0 by 3 to 10 times (the mean value is $N_m/N_0 = 4.5$). The most probable time of the NB beginning is 10–11 a.m. of local time, and the duration is 7 hours.

The disperse composition of near-ground aerosol in the days with NB differs from the background one by the appearance of the nucleation mode with $D = 3$ to 20 nm (for a comparison see the mean aerosol spectra in Fig. 4).

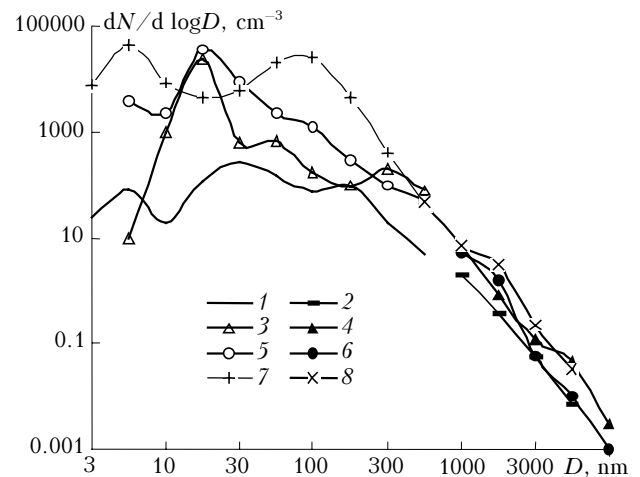


Fig. 4. Aerosol size distributions characteristic of weakly (1, 2) and moderately (3–8) turbid near-ground layer. Curves 1 and 2 are episode of NB, March 25, 2000, 10 a.m.; curves 3 and 4 are April 4, 2000, since 6 until 9 a.m.; curves 5 and 6 are episode of NB, April 4, 2000, noon; curves 7 and 8 are measurements in Moscow region, morning, summer 1990–2000. The data 1 are obtained by means of the DMPS spectrometer, 3, 5, and 7 – by means of the DAES-2 analyzer, 2, 4, 6, and 8 – by means of the PC-218 counter.

As is seen, the Aitken mode particles $D = 40–80 \text{ nm}$ also show noticeable variations in these days, their size is sufficient for acting as cloud condensation nuclei. The rate of the nuclei growth in the first two hours after the beginning of NB is absent, and variations of the coarse particle fraction $N_a = 0.5–5 \mu\text{m}$ are small.

The data happened to be unexpected on the correlation between the dynamics of small particle number density $D < 100 \text{ nm}$ and the initial number density of coarse aerosol. The diagrams of the diurnal behavior of the total aerosol and intermediate ions number densities and concentrations of trace gases in two specific days with small (April 2, 2000) and moderate (March 29, 2000) initial turbidity of air are shown in Fig. 5. Meteorological and synoptic conditions during these two days were identical, but scenarios of the development of aerosol were different. In the first case the “classic” aerosol system with Aitken mode of $D = 40–80 \text{ nm}$ and cumulative mode with $D = 100–200 \text{ nm}$ was formed in practically dustless air during 6–7 hours. In the second case, the nucleation mode of $D = 3–10 \text{ nm}$ only joined to similar but earlier formed system for the time period of 6–7 hours.

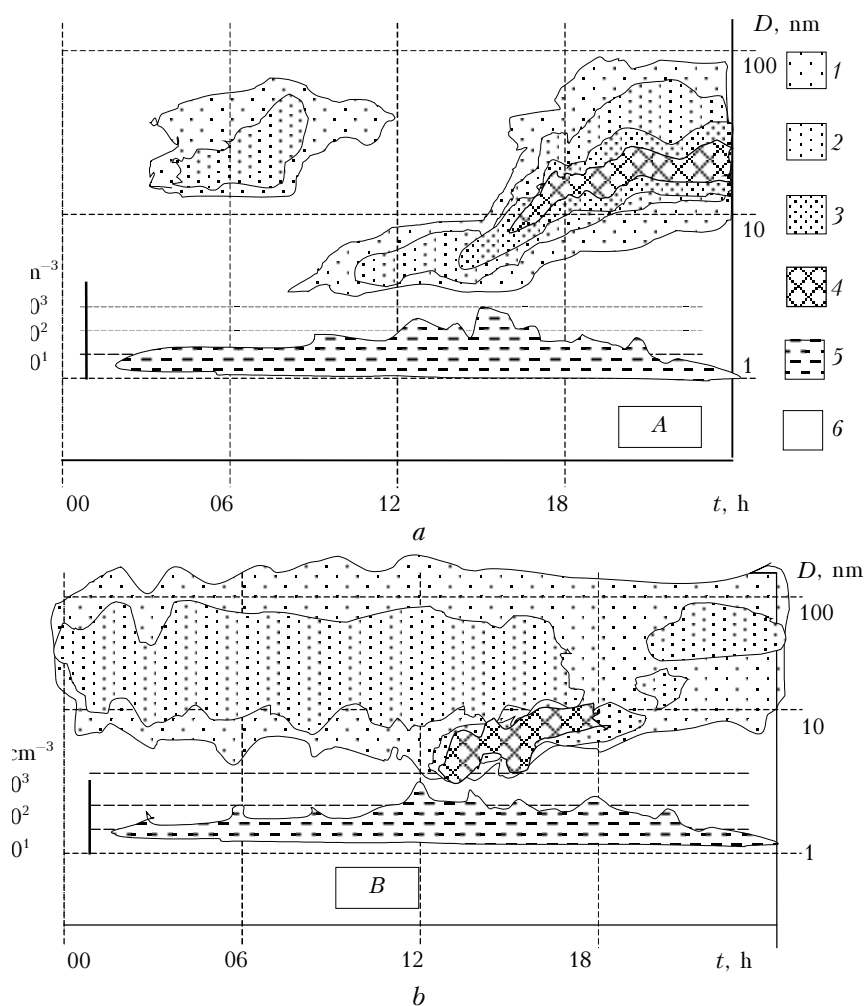


Fig. 5. Diagrams of diurnal variations of aerosol, intermediate ions, and trace gases at weak (*a*) and moderate (*b*) air turbidity. Curves 1–4 are number density of aerosol of the diameter $D = 3$ to 100 nm: more than $5 \cdot 10^2 \text{ cm}^{-3}$ (1); more than 10^3 cm^{-3} (2); more than $5 \cdot 10^3 \text{ cm}^{-3}$ (3); more than $5 \cdot 10^3 \text{ cm}^{-3}$ (4) but without charger; number density of intermediate ions M_{\pm} (5, left scale); the cases of noticeable exceeding of gas concentrations over the background value (6): $[\text{SO}_2] = 0.5\text{--}0.75$ ppb, $[\text{NO}_x] = 0.75\text{--}1.5$ ppb (A); $[\text{SO}_2] = 1\text{--}1.75$ ppb, $[\text{NO}] = 0.25\text{--}0.75$ ppb, $[\text{NO}_x] = 3\text{--}5$ ppb (B).

The case of weakly turbid air (25% of events). This case is illustrated in Fig. 5*a*. The number density of Aitken mode and cumulative mode particles varied before the beginning of NB within the limits $N_0 = 500$ to 1000 cm^{-3} . The number density of coarse particles did not exceed the value of the order of $N_a = 1 \text{ cm}^{-3}$. Generation of new particles started at the noon, by this time the number density of the nucleation mode particles decreased to zero and the total number density of particles was about 500 cm^{-3} , principally due to the particles of cumulative fraction. Formation of the nucleation mode occurred during 1–2 hours. Particles grew gradually, the Aitken nuclei fraction with $D = 100\text{--}200$ nm was formed by 3 p.m., and the cumulative fraction was formed by 6 p.m. (see Fig. 4, curves 1 and 2, and Fig. 5*a*). The changes did not touch the coarse aerosol distribution, which had Junge shape with the index 3.5. The number density of the particles of this fraction remains at a comparatively low level $N_a < 1 \text{ cm}^{-3}$. The wind velocity at the height of 67 m in this period did not

exceed 3–4 m/s, and the wind direction changed from 0 to 90° . Relative humidity reached the minimum of 25% by 3 p.m. The aerosol number density reached maximum of $N = 5000 \text{ cm}^{-3}$ approximately by 5 p.m. As is seen in Fig. 5*a*, the nucleation mode was not observed. The single-mode distribution with the maximum in the region of Aitken mode (close to curves 1 and 2 in Fig. 4) was observed until next morning.

The case of moderately turbid air (35–40% of events). As is seen in Fig. 5*b*, new particles of nanometer size range began to appear at 9–10 a.m. The number density of particles of the nucleation mode reached its maximum at noon. The initial number densities of particles with the diameter of 3 nm and greater lied in the range $N_0 = 2000\text{--}20000 \text{ cm}^{-3}$, and that of coarse particles was $N_a = 1\text{--}2 \text{ cm}^{-3}$. The Aitken, with $D = 40\text{--}80$ nm and cumulative with $D = 100\text{--}200$ nm particles were well pronounced in the initial spectrum (see Fig. 4), their positions remained the same at the increase of the total number density of

particles up to 20000 cm^{-3} at noon. The nucleation mode, that contained up to 80% of new particles, gradually dissipated by 4–5 p.m. Then the shape of the particle size spectrum reconstructed. The total number density of particles decreased by the evening to the initial value of 2000 to 3000 cm^{-3} .

It is useful to note that the low and moderate turbidity of air is characteristic of not only transitional seasons at the Hiitila Observatory, Southern Finland. For a comparison, the mean number density of particles of the diameter greater than $0.5 \mu\text{m}$ in the Finnish part of Lapland in 1992–95 did not exceed 1.5 cm^{-3} , and the number density of particles³¹ in the size range $D = 0.3\text{--}0.5 \mu\text{m}$ did not exceed 10 cm^{-3} . As to the other peculiarities of the aerosol climate of Finland, let us note that the values N_0 and N_a in the near-ground atmosphere of mid-latitudes^{4,10} and even some sub-polar regions¹¹ are greater than that in the air basin of Hiitila Obs. The nucleation and cumulative modes also are observed in forests of Moscow region (curves 7 and 8) at morning inversions, though the Aitken mode is not pronounced. According to the model,¹⁰ summer smog of natural origin is responsible for the intense morning peaks of the number density of particles of nucleation mode in deciduous forests of Moscow region. Different from coniferous forests of Finland, the nucleation mode was practically never observed in Moscow region in the afternoon.

The case of turbid air (25–35% of events). Nucleation bursts were not observed at the increase of the near-ground aerosol number density $N_0 > 2000 \text{ cm}^{-3}$, $N_a > 2 \text{ cm}^{-3}$. Let us note that the revealed threshold does not contradict the experimental estimate of the NB threshold by the total area of particles²¹ $S < 100 \mu\text{m}^2/\text{cm}^3$.

Thus, the “aerosol” state of the atmosphere is a very essential factor of the NB appearance. In particular, high values of the intensity of nucleation N_m/N_0 are characteristic of the lower number densities of aerosols of the diameter greater than $0.5 \mu\text{m}$, and the threshold of appearance of NB unambiguously corresponds to the condition $N_a < 2\text{--}3 \text{ cm}^{-3}$. At the same time, no noticeable correlation is observed at low turbidity between the parameter N_m/N_0 , the time of beginning of NB t_0 , their duration t , and the aerosol number density. We also have not succeeded in revealing any reliable relations between N_m/N_0 , t_0 and t , and concentration of the considered trace gases. Low turbidity of air is, evidently, the necessary factor, but obviously insufficient, because the phenomena of NB were not observed in the nighttime (see, for example, Fig. 5a) as well as in 20% of events in the daytime.

According to the ideas from Refs. 12, 17, and 23, one can obtain some answers to the questions about the genesis of NB from the detailed analysis of electric interactions in the atmosphere.

3.3. Electric state of the air

It follows from Table 2 that the background (before the NB episodes) electric conductivity of the

air $C = (C_+ + C_-)/2$ was, on the average about $12 \pm 2 \text{ fCm/m}$. This is 25–35% greater than the values characteristic of the center of European part of Russia.^{6,8} The coefficient of unipolarity C_+/C_- was close to the equilibrium value of 0.95–1.1, and the strength of the electric field was in the limits 100–250 V/m. Such values make it possible to characterize the electric state of the near-ground atmosphere during NB as a quasi-neutral and close to the mean global one.²⁰

The relations between the peak number densities of particles N_m generated in the NB episodes and the principal mobility groups of the atmospheric ions: light n , intermediate M_+ , M_- , m_- , and heavy N_- are shown in Fig. 6.

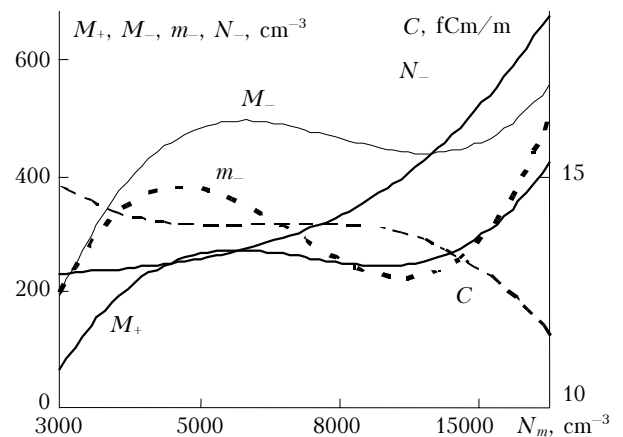


Fig. 6. Statistical relations of the maximum number density of new aerosols N_m with the mean electric conductivity of air and number densities of ions M_+ , M_- , m_- , and N_- during NB. Notations are in Table 1. The data of measurements are approximated by polynomials of the third degree.

The mobility values of the groups are presented in Table 1. One can see that the nucleation bursts were accompanied by unambiguous increase of the number densities of intermediate and heavy atmospheric ions. The number density of light ions n_- and polar electric conductivity C of the air are more conservative, but they decreased by 30–40% at the intense NB ($N_m > 5 \cdot 10^3 \text{ cm}^{-3}$) (Figs. 3d and 6). One can qualitatively explain these results by the decrease of the intensity of ion formation due to the daytime decrease of the radon concentration (Fig. 3a) and the increase of the aerosol cross section of light ions adsorption.

It is also logical to relate the variations of heavy ions (Figs. 3 and 6) with variations of the total number density of atmospheric aerosols N . If variations of N have been quite slow and the Boltzmann charge distribution has been realized (see, for example, Refs. 20 and 26), the number densities of heavy ions of both signs N_+ , N_- follow the total number density of particles N approximately proportionally. The characteristic time of ion charging of submicron aerosols at the ranges of the light ion number density of both signs observed at Hiitila Obs. $n_+ = n_- = 500\text{--}800 \text{ cm}^{-3}$ is of the order of some hours, that corresponds to the real time scale of NB evolution.

As the issue of the degree of stationarity and equilibrium of electric processes is important, in principle, special experiments have been conducted. The bipolar charger of the aerosol spectrometer DMPS was switched off, i.e., the device passed to the regime of highly sensitive analyzer of electric mobility of heavy ions in the range from 0.25 to $2.5 \cdot 10^5 \text{ cm}^2/\text{V} \cdot \text{s}$. Electric mobility of particles charged in natural bipolarly ionized air were analyzed. This regime is seen in Fig. 4 as an approximately twofold decrease of the range, to which the particles of nucleation mode mostly contribute, i.e., the conditions of electric equilibrium in air were reached for the particles with $D < 5 \text{ nm}$, and were not reached for larger particles ($D = 10$ to 50 nm), however only under condition that the number density of the latter exceeded $5 \cdot 10^3 \text{ cm}^{-3}$. The ratio of the number densities of particles at switched off and switched on bipolar charger $N_{\text{off}}/N_{\text{on}}$ changed in different days from 0.2 to 1. This ratio in measurements of April 2, 2000 is close to 0.9, that is explained by small value of the total content of aerosol and the small rate of growth at a sufficiently high electric conductivity of the air. The deviations from electric equilibrium in measurements on March 29, 2000 were quite large: $N_{\text{off}}/N_{\text{on}} = 0.2\text{--}0.3$.

The analysis of diurnal variations provides for useful information about the relations of the number densities of aerosols, N , and intermediate ions, M . It was already noted that the maxima of number densities of new particles N and ions M can coincide as in Fig. 5b, or not coincide as in Fig. 5a with the maximum of solar radiation. In the second case, the delay was 3 and 6 hours for intermediate ions and aerosols, respectively. The maximum M was most often observed at a time when the air was maximum heated and well mixed, and the process of aerosol formation was still intense. This means that, analogous to the laboratory experiments,^{7–9} an intense generation of new aerosol particles stimulates the process of disappearance (most likely, due to adsorption) of not only light but also intermediate ions. Quantitative analysis of the corresponding features is beyond of the frameworks of the present investigation.

Conclusions

1. Formation of aerosol particles of a nanometer size, $D = 3$ to 20 nm , which form the so-called nucleation size fraction with the number density of particles from $3 \cdot 10^3$ to $20 \cdot 10^3 \text{ cm}^{-3}$ can occur in the near-ground atmosphere in spring and fall seasons in daytime. This fraction lives during few hours. Then particles can grow inside the Aitken fraction 40 to 80 nm and cumulative fraction 100 to 200 nm . The characteristic time of the beginning of such a process is 11 a.m., and the duration is about 7 hours.

2. The important and statistically significant result of our observations is that the formation of atmospheric ions of the medium mobility from 0.5 to $0.05 \text{ cm}^2/\text{V} \cdot \text{s}$ precedes each appearance of nanometer particles. On the contrary, intense generation of aerosol particles leads to disappearance of intermediate

ions. Perhaps, intermediate ions and the products of their association then play the role of primary nuclei.

3. The essential factor of appearance of new particles is the “aerosol” state of the atmosphere. In particular, high values of the nucleation rate N_m/N_0 are characteristic of small values of the aerosol number density of the diameter greater than $0.5 \mu\text{m}$, and the threshold of appearance of the NB unambiguously corresponds to the condition $N_a < 2\text{--}3 \text{ cm}^{-3}$. At the same time, no noticeable correlation is observed at low turbidity between the parameter N_m/N_0 , the time of beginning of NB, t_0 , their duration t , and the aerosol number density. Low turbidity of air is, evidently, the necessary factor, but obviously insufficient, because the NB phenomenon was not observed in the nighttime (see, for example, Fig. 5a) as well as in some events in the daytime.

Thus, the role of daytime solar heating stimulating the entrance of low turbid air to the near-ground layer is obvious for understanding the mechanism of emission of new particles.

4. The intensity of nucleation N_m/N_0 does not directly and unambiguously depend on the observed concentrations of nitrogen and sulfur oxides. The latter undergo synchronous and strong fluctuations, which do not overstep the limits of natural diurnal variations. The values of N_m/N_0 are minimum at the winds from the south. Nevertheless, it should be logical to assume the inverse dependence, because, according to Ref. 28, winds from south bring different pollutants to Scandinavia from Europe, in particular, the smog-producing gases and dust. We also have not succeeded in revealing any reliable relations between N_m/N_0 , the time of beginning, t_0 , and the duration of emissions t . These facts, as well as the absence of correlation between the intensity of NB and the concentrations of SO_2 , NO , and NO_x force us to think about some principal factors of NB concerning their genesis and intensity. If one follows numerous photochemical and biogenic models of aerosol generation (see, for example, Ref. 1), it is logical to propose the increase in the content of nitrogen and sulfur oxides as well as of the products of forest vital activity to be the factors favoring the NB appearance. However, analysis of Figs. 1–3 shows only some factors of these models. Next, the NB events are observed only in sunny days; in daytime the concentrations of O_3 , SO_2 , CO_2 , NO , and NO_x gases sometimes increase, and the near-ground ozone concentration increases in spring (see Fig. 2).

Other facts are statistically more reliable. First, emissions of new particles are observed most often in early spring and in late fall, i.e., when the yield of bioproducts is minimum. The maximum of biogenic substances in the atmosphere is usually observed in summer when the NB phenomena are quite rare. Second, the yield of biogenic products significantly prevails in the nighttime, but not in the midday, when emissions of new particles occur. Third, we have not revealed any explicit dependences of the number density of new particles on the concentrations of such smog-producing gases as ozone, carbon dioxide, nitrogen and sulfur oxides.

Taking into account the results obtained, one can conclude that the detailed consideration of the formation of ion and aerosol spectra in the near-ground layer, knowledge of the vertical profiles of meteorological and other parameters, at least, up to 300 m will be important for further investigations.

Acknowledgments

The work was supported in part by Grants No. 4622 and No. 5387 of Estonian Scientific Foundation.

References

1. K.Ya. Kondratyev and D.V. Pozdnyakov, *Aerosol Models of the Atmosphere* (Nauka, Moscow, 1981), 104 pp.
2. K.P. Koutsenogii and A.I. Smirnova, *Atmos. Oceanic Opt.* **14**, Nos. 6–7, 463–467 (2001).
3. I.P. Vetlov and N.F. Vel'tischev, eds., *Handbook on the Use of Satellite Data in Weather Analysis and Forecast* (Gidrometeoizdat, Leningrad, 1982), 299 pp.
4. M.V. Panchenko and V.V. Pol'kin, *Atmos. Oceanic Opt.* **14**, Nos. 6–7, 478–488 (2001).
5. D.E. Pozdnyakov, in: *Secondary Aerosols, or Aerosols Formed in Situ* (Gidrometeoizdat, Leningrad, 1991), pp. 141–190.
6. J. Salm, in: *Chemistry of Plasma*, Issue 17, 194–217 (1993).
7. V.V. Smirnov, *Izv. Ros. Akad. Nauk, Fiz. Atmos. Okeana* **28**, No. 9, 958–966 (1992).
8. V.V. Smirnov, *Ionization in the Troposphere* (Gidrometeoizdat, St. Petersburg, 1992), 312 pp.
9. V.V. Smirnov, *Trudy Ins. Exp. Meteorol.* Issue 30 (104), 76–106 (1983).
10. V.V. Smirnov, *Meteorol. Gidrol.* No. 9, 18–27 (2003).
11. V.V. Smirnov, A.A. Pronin, V.F. Radionov, A.V. Savchenko, and V.P. Shevchenko, *Izv. Ros. Akad. Nauk, Fiz. Atmos. Okeana* **36**, No. 5, 639–649 (1999).
12. V.V. Smirnov, J. Salm, J.M. Mäkelä, and J. Paatero, in: *Proc. of 5th Russian Conference on Atmospheric Electricity* (Vladimir, 2003), pp. 127–130.
13. K.F. Tammet, *Scientific Letters of Tartu State University* (1967), 82 pp.
14. R.R. Khairullin, *Maps of Synoptic Characteristics of Cyclo- and Anticyclogenesis and Cyclo- and Anticyclolysis in Northern Hemisphere* (Obninsk, 1990), 83 pp.
15. G. Buzorius, Ü. Rannik, J.M. Mäkelä, T. Vesala, and M. Kulmala, *J. Aerosol Sci.* **29**, 157–171 (1998).
16. G. Buzorius, Ü. Rannik, D. Nilsson, and M. Kulmala, *Tellus* **53B**, 394–405 (2000).
17. J. Haataja and T. Vesala, eds., *SMEAR II. Station for Measuring Forest Ecosystem – Atmosphere Relation* (Aseman Kir., Orivesi, Finland, 1997), 100 pp.
18. U. Hörrak, J. Salm, H. Tammet, *J. Geophys. Res.* **103**, 13909–13915 (1998).
19. U. Hörrak, F. Miller, A. Mirme, J. Salm, and H. Tammet, in: *Scientific Letters of Tartu State University*, No. 880, 33–42 (1990).
20. H. Israëli, *Atmospheric Electricity* (Israel Program for Sci. Translations, Jerusalem, 1973), Vol. 2, 796 pp.
21. M. Kulmala, K. Hämeri, J.M. Mäkelä, et al., *Boreal Env. Research* **5**, No. 4, 281–297 (2000).
22. J.M. Mäkelä, M. Dal Maso, L. Pirjola, P. Keronen, L. Laakso, M. Kulmala, and A. Laaksonen, *Boreal Env. Research* **5**, No. 4, 299–314 (2000).
23. J.M. Mäkelä, J. Salm, V.V. Smirnov, I. Koponen, J. Paatero, and A.A. Pronin, in: *Proc. of 12th Intern. Conf. on Atmospheric Electricity* (Versailles, France, 2003), pp. 793–796.
24. J.M. Mäkelä, I.K. Koponen, P. Aalto, and M. Kulmala, *J. Aerosol Sci.* **31**, 595–611 (2000).
25. J.M. Mäkelä and V.V. Smirnov, in: *Intern. Aerosol Conf. to Memory Prof. A. Sutugin* (Moscow, 2000), pp. 156–157.
26. J.M. Mäkelä, J. Salm, V.V. Smirnov, I. Koponen, J. Paatero, and A.A. Pronin, *J. Aerosol Sci.* **32**, S149–S150 (2001).
27. V.V. Smirnov and J.M. Mäkelä, in: *Proc. of 12th Intern. Conf. on Atmospheric Electricity* (Versailles, France, 2003), pp. 397–397.
28. V.V. Smirnov, in: *Intern. Aerosol Conf. to Memory Prof. A. Sutugin* (Moscow, 2000), pp. 219–220.
29. V.V. Smirnov, A.V. Savchenko, and A.A. Pronin, *J. Aerosol Sci.* **29**, Suppl. 1, S875–S876 (1998).
30. T. Vesala, J. Haataja, P. Aalto, N. Altimir, G. Buzorius, E. Garam, K. Hämeri, H. Ilvesniemi, V. Jokinen, P. Keronen, T. Lahti., T. Markkanen, J.M. Mäkelä, E. Nikinmaa, S. Palmroth, L. Palva, T. Pohja, J. Purnpanen, U. Rannik, E. Siivola, H. Ylitalo, P. Hari, and M. Kulmala, *Trends in Heat, Mass & Momentum Transfer* **4**, 15–35 (1998).
31. A. Virkkula, R.E. Hillamo, V.-M. Kerminen, and A. Stohl, *Boreal Env. Research* **2**, 317–336 (1997).
32. H.C. Willett, *J. Geophys. Res.* **67(2)**, 661–670 (1962).
33. W. Winklmayr, G.P. Reischl, A.O. Lindner, and A. Berner, *J. Aerosol Sci.* **22**, 289–296 (1991).